The Effects of Cerium and Titanium Additions on Hot Cracking in Welds of a Cr-Mo-V Rotor Steel

The cause of the hot cracking and a means of preventing it are established

BY A.-L. LU, S. Y. YOO AND A. W. PENSE

Introduction

The Cr-Mo-V steels have been frequently used for turbine rotors in power generation facilities because of their superior high-temperature properties. When such a rotor fails during service due to cracking from fatigue, creep, or stress corrosion, there are several options one can take. One is to replace the rotor with a new one, which is the traditional approach. Another, now being used more commonly, is to repair the rotor using welding. The latter approach is considered increasingly feasible as welding techniques for rotor materials are developed, and it is attractive because the costs of weld repairs are significantly less than those of replacement.

One of the difficulties in this kind of welding is the potential susceptibility of the rotor steel to various kinds of cracking. This investigation, which is part of a larger program on rotor steel welding (Ref. 1), concerns hot cracking and its mitigation. Hot cracking is a form of cracking that occurs during solidification of the weld. As the solidifying metal contracts, stress is applied across and between weld metal dendritic crystals. Interfaces between these dendrites, especially those with liquid films on them, separate under the applied stress and produce macroscopic cracking. The tendency for cracking is therefore increased when alloy elements that promote the formation of low-melting liquid films are present. Other forms of cracking may also be of concern in these steels, such as delayed cracking or stress relief cracking. However, this paper is concerned with hot cracking.

The steel in this investigation is a Cr-Mo-V steel made with air melt technology in the 1950's and retired after 17 years of service. It has a high-residual alloy element content, as was typical of many steels produced in that time period, and has a high-carbon content for welding. Many residual elements, especially S, are reported to promote hot cracking in steel weldments. The presence of Mn in steels is known to mitigate the effects of S; however, the Mn/S ratio for this steel is only 26, a value considered low enough to be of some concern. Moreover, in the weld repair of rotors, some procedures call for gas tungsten arc root passes. These passes are often autogenous, and thus, the base metal composition serves as that of the weld metal. It is under these circumstances that weld cracking is most likely.

Modification of cracking by site additions is one approach to this problem and is the one investigated here. Certain types of additions can change the chemical form of the impurity elements so they are less harmful, and may alter the solidification pattern so it is less favorable to cracking. Both of these effects are possible with the site additions of Ce and Ti (Ref. 2). The results of the study are intended to provide potential ways to improve the quality of rotor welding, and especially repair welding.

KEY WORDS

Cr-Mo-V Rotor Steel
Cerium + Titanium
Ce-Ti Additions
Weld Hot Cracking
Crack Susceptibility
Cr-Mo-V Hot Cracking
Rotor Steel Repair
Varestraint Testing
SEM + EPMA Analyses
TEM + STEM Analyses

A.-L. LU is a visiting Research Scholar, S. Y. YOO is a Graduate Student and A. W. PENSE is a Professor and Associate Dean, College of Engineering and Physical Sciences, Lehigh University, Bethlehem, Pa.

Based on a paper presented at the 67th Annual AWS Convention, held April 13-18, 1986, in Atlanta, Ga.

Materials and Procedures

Materials Used

The effects of cerium and titanium on the hot cracking of an older Cr-Mo-V turbine rotor were investigated using a steel that has the chemical composition and mechanical properties shown in Table 1. As indicated before, its C content, at 0.36%, is somewhat high for easy welding. The residual P and S content, 0.032% and 0.039%, respectively, is high by modern standards. Its alloy content is

Table 1—Chemical Analysis and Mechanical Properties of the Cr-Mo-V Steel

Chemical Analysis (wt-%)								
C	Mn	P	S	Si	Ni	Cr	Mo	V
0.36	0.83	0.032	0.039	0.30	0.13	0.95	1.25	0.24

Mechanical Properties							
Yield		Tensile		Elong.	Trans. Temp.		K_{Ic}
MPa	(ksi)	MPa	(ksi)	%	°C	°F	MPam½
630	91.4	806	117.0	20	310	590	37

Table 2—Added and Recovered Amounts of Cerium and Titanium

Specimen Group	Ce, % Added	Ce, % Recovered	Ti, % Added	Ti, % Recovered
BOV	–	–	–	–
B1C	0.07	0.007	–	–
B2C	0.15	0.014	–	–
B3C	0.25	0.029	–	–
B4C	0.45	0.047	–	–
B1T	–	–	0.05	0.026
B2T	–	–	0.10	0.044
B3T	–	–	0.15	0.053
B4T	–	–	0.30	0.11

also rather high for good weldability. Yield and tensile strength are typical of heat-treated steels, and its toughness, as measured by its transition temperature and ambient temperature fracture toughness, is low. The Ce and Ti materials used for additions were made in the form of foils 0.25 mm (0.010 in.) thick having compositions of 99.7% Ce and 99.9% Ti, respectively.

Specimen Preparation

The hot cracking susceptibility of the steel was studied using the Rensselaer Polytechnic Institute (RPI) Varestraint test. The preparation of specimens with site additions was accomplished as follows. The Ce and Ti foils were cut into strips and weighed with a precision balance to produce the addition levels desired. The strips were then sealed in a seamless low-carbon tube with an outer diameter of 3.2 mm (0.12 in.) and an inner diameter of 2 mm (0.08 in.). The tubes were pressed flat and laid in a premachined groove in the Varestraint specimen. A pretest melting procedure was performed with the gas tungsten arc process producing a melted alloy layer in the groove. The specimen was ground flat prior to Varestraint testing. While welding the Ce-containing specimen, care was taken to avoid oxidation. The nominal amounts of the Ce and Ti added are listed in Table 2, along with the actual amounts recovered as determined by analysis. It should be noted that, in spite of some care, the recovery of Ce was only about 10% and of Ti was about 30–50%.

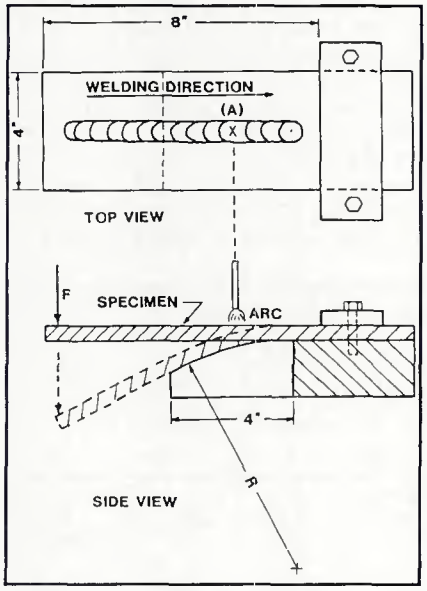

Fig. 1—RPI Varestraint test

Varestraint Tests

The Varestraint tests were conducted to determine the susceptibility of the Cr-Mo-V steel to hot cracking and to compare the effect of Ce and Ti as site additions to increase its resistance to hot cracking. The Varestraint test apparatus was developed in the welding laboratory at Rensselaer Polytechnic Institute to evaluate cracking susceptibility, particularly hot cracking susceptibility, of metals (Ref. 3). The important details of the procedure are shown schematically in Fig. 1. The specimen is clamped in the machine directly under the welding arc. As the arc passes the point marked A in Fig. 1, a pneumatically activated loading yoke bends the specimen downward suddenly to conform to the radius, R, of a removable die block. The radius of the block controls the applied strain, called the augmented strain. After the test, the surface of the specimen is examined for cracking and the total length of surface cracks is recorded.

The specimens tested were the standard size, 300 × 50 × 12.5 mm (12 × 2 × 0.5 in.). To maintain the identical conditions while testing the steel with no site additions, empty tubes were prewelded into these specimens. The GTAW process was used for the Varestraint tests. To protect the resulting crack surfaces from oxidation, an auxiliary shielding nozzle was used. In order to emphasize the results of the tests, a relatively large augmented strain, 4%, and a high heat input, 2.8 kJ/mm (72 kJ/in.) were used. Parameters used in the Varestraint test welds are listed in Table 3. The total crack length produced in the tests measured at 100X magnification was used as the criterion to assess the tendency to hot cracking. For every condition tested, three specimens were used.

Table 3—Varestraint Test Conditions

Current	320 A (DC)
Voltage	15 V
Travel Speed	100 mm/min (4 ipm)
Electrode	3.18 mm (0.125 in.) dia. 2% thoriated W, 90 deg
Arc Length	2.4 mm (0.094 in.)
Gas Flow	28 L/min (40 ft^3/h)

Measurements of Dendrite Arm Spacing

For determining the influence of the different additions on the solidification structure of the weld metals, the primary dendrite arm spacing was measured on cross-sections cut from the Varestraint specimens. The measurements were performed with an optical microscope at a magnification of 200X. It is known that there are some differences in crystallization patterns between the center and bottom of the weld bead. This is because the bottom solidifies faster than the center, and the resulting columnar crystals grow in a curved pattern. In addition, there is a difference in constitutional supercooling between these two areas.

Thus, measurement of primary arm spacing was performed in both the center and bottom parts of the weld nugget. Standard procedures for grain-size measurement were utilized (Ref. 4); however, since dendrites of the weld metals have a preferential growth orientation, the measuring line, while randomly positioned, was always oriented perpendicular to the elongated axes of the dendrites. At least ten fields were measured on every cross-section, and three cross-sections were measured for each weld.

Scanning Electron Microscope and Surface Chemical Analysis

The characteristics of the crack surfaces and the compositions of the segregated phases on them were analyzed with a scanning electron microscope (SEM) equipped with an energy dispersive spectrum analysis (EDS) system. To expose the surfaces of select cracks in the Varestraint specimens, notches were made at their tips. The specimens were then cooled in liquid nitrogen and broken open by impact. To reveal elemental segregation on the surfaces, an electron microprobe analysis technique (EPMA) was used on polished samples etched with sodium bisulfide solution.

Transmission Electron Microscope Analysis

Transmission electron microscopy (TEM) and scanning transmission electron

Table 4—Effect of Ce and Ti Additions on Total Crack Length

Specimen Type	Ce or Ti Content (%)	Total Crack Length[a] (mm)
BOV	–	31.0
B1C	Ce 0.007	22.3
B2C	Ce 0.014	16.4
B3C	Ce 0.029	22.5
B4C	Ce 0.047	28.8
B1T	Ti 0.026	25.2
B2T	Ti 0.044	20.2
B3T	Ti 0.053	22.7
B4T	Ti 0.11	27.6

(a) Average value.

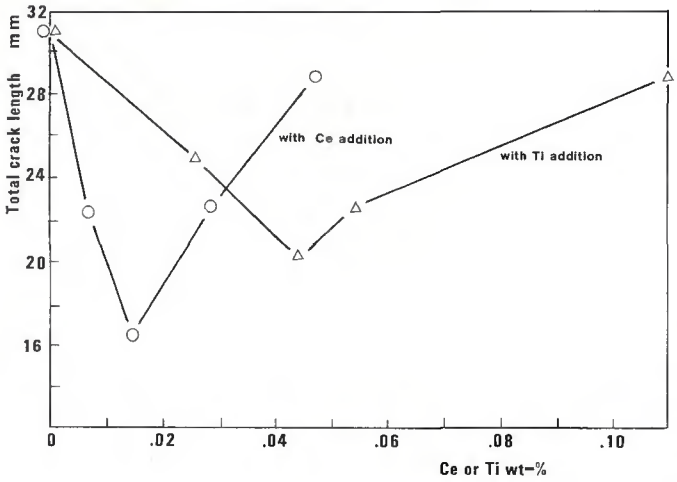

Fig. 2—Effects of cerium and titanium additions on total crack length

microscopy (STEM) were employed for analysis of fine structures and chemical compositions of the intergranular segregated phases in weld metal samples with different additions. Direct carbon extraction replicas were used for this purpose. The very high resolution of the STEM using EDS analysis makes it possible to find some fine differences in chemical composition between the phases at grain boundaries in different weld metals.

Because copper grids were always used for holding the replicas, there were always copper peaks on the spectrum profiles, and copper was, therefore, not considered in the analysis.

Results

The Effects of Ce and Ti on Hot Cracking

As mentioned above, the Varestraint tests of the Cr-Mo-V rotor steel with different additions were conducted using a high heat input and at a high augmented restraint level. The results of these tests are shown in Table 4 and Fig. 2. With respect to the base cracking level measured for this steel, it is not possible to relate this to an absolute level of weldability; however it can be compared to five other rotor steels in the Lehigh program (Ref. 1). The total crack lengths measured for these steels tested under similar circumstances varied from 3.7 to 34.1 mm (0.14 to 1.34 in.). Thus, the Buck rotor steel, at a total crack length of 31.0 mm (1.22 in.), was one of the more crack-sensitive materials.

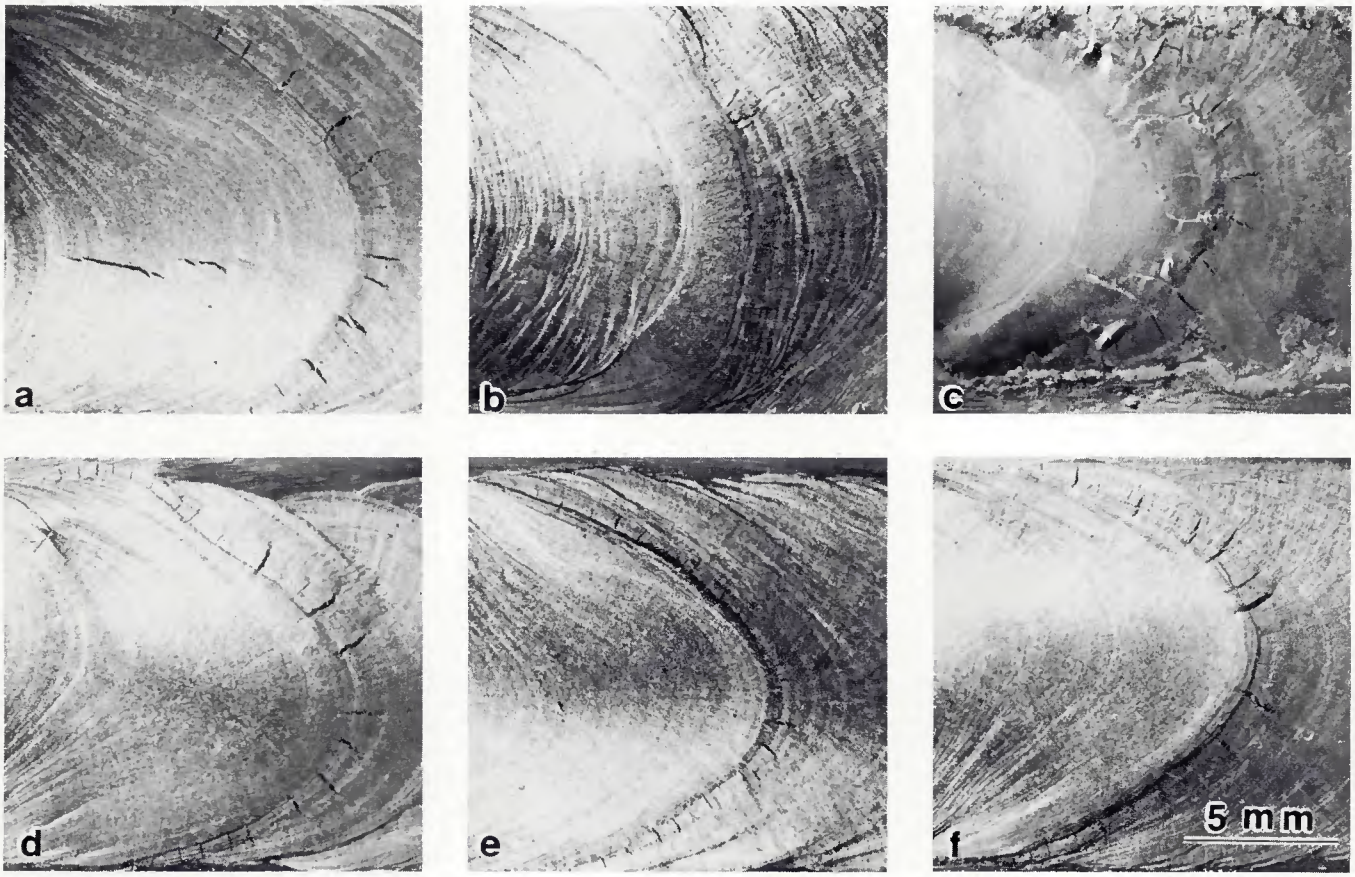

Fig. 3—Changes in crack appearance of the Varestraint specimens with different additions. A—No additions; B—0.014% Ce; C—0.047% Ce; D—0.026% Ti; E—0.044% Ti; F—0.11% Ti

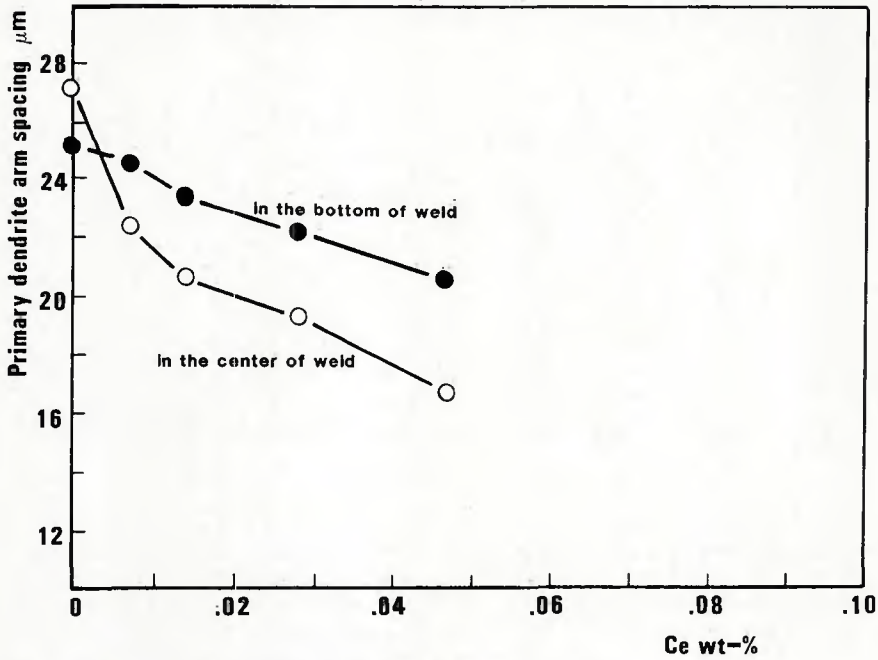

Fig. 4—Effects of cerium additions on primary dendrite arm spacing

As can be seen from Fig. 2, Ce and Ti have strong effects on the susceptibility to hot cracking, and the effects are not monotonic. Both Ce and Ti have their own optimum level with respect to hot crack resistance. Crack susceptibility is lowest when Ce is within 0.01-0.03% and Ti is within 0.03-0.06%. In these ranges, Ce reduces the cracking sensitivity to about 55% of its original level and Ti reduces it to about 70%. Figure 3 shows the change in appearance of the cracks with Ce and Ti content. These photographs are a plan view of the specimen's welded surface.

Effects of Ce and Ti on Solidification Structure

The measurements of the primary arm spacing of dendrites indicate that both cerium and titanium can effectively reduce the primary arm spacing. In other words, they can refine the crystallization structure of the welds. The results of the measurements are shown in Table 5 and Figs. 4 and 5. A very interesting observation is that the effects of Ce and Ti are different. The Ce seems to reduce the dendrite arm spacing effectively in the center part of the cross-section of the weld. The Ti, however, seems rather to refine the dendrites in the bottom part of the cross-section and to alter the preferred orientation of the columnar dendrites. These features are shown in Figs. 4-6.

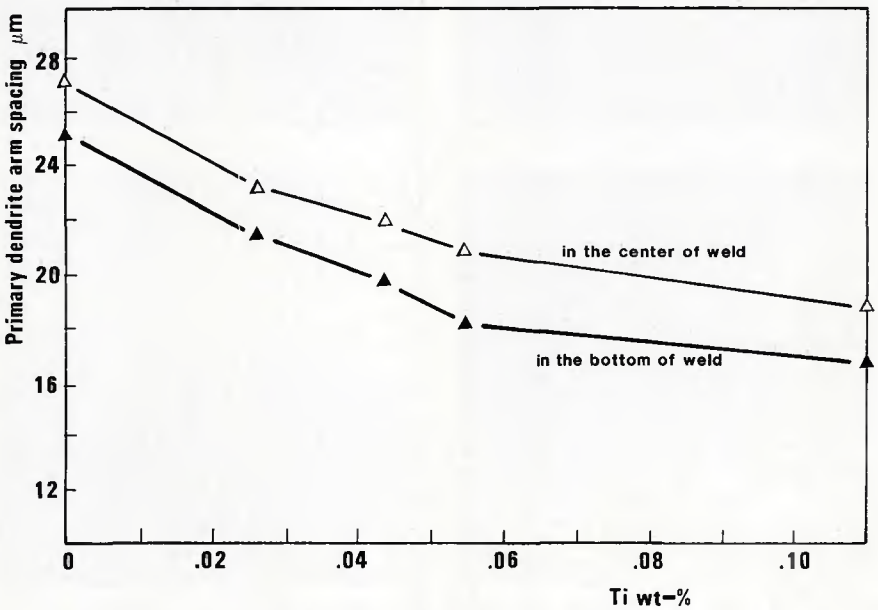

Fig. 5—Effects of titanium additions on primary dendrite arm spacing

Table 5—Effects of Ce and Ti Additions on Primary Dendrite Arm Spacings

Specimen Type	Center Arm Spacing (m)	Bottom Arm Spacing (m)
BOV	27.2	25.5
B1C (Ce)	22.1	24.5
B2C (Ce)	20.8	23.6
B3C (Ce)	18.7	22.1
B4C (Ce)	16.7	20.7
B1T (Ti)	23.1	21.6
B2T (Ti)	22.1	20.2
B3T (Ti)	20.8	18.0
B4T (Ti)	18.9	16.9

Effects of Ce and Ti on Interdendritic Phases

The results of SEM and SEM/EDS analyses of the crack surfaces of the weld with different additions are shown in Figs. 7 and 8. The EPMA results on the interdendritic particles in the welds with 0.047% Ce addition are shown in Fig. 9. Figures 10-12 show the results of TEM and STEM/EDS analyses.

Typical "rock cave" features can be observed at low magnification on the crack surfaces of the weld metal with no additions—Fig. 7A. At high magnification, considerable amounts of segregated phase can be seen as continuous interdendritic films—Figs. 7B and 10A. The SEM/EDS analyses indicate that these film-like interdendritic phases have high S and Fe contents—Fig. 8A. The STEM/EDS analyses also reveal that some parts of the interdendritic films are enriched by S and Fe—Fig. 11A, and other parts are enriched with Mo, V and Cr—Fig. 11B. This is evidence of substantial segregation of both S and C at the dendrite boundaries. It is clear that the interdendritic films are mainly sulfides, sometimes accompanied by carbides.

On the crack surface of the weld with 0.014% Ce, most of the interdendritic phases have become round and rod-like—Figs. 7C, 7D and 10B. The SEM/EDS analyses indicate that they have high S and Ce contents—Figs. 8B and 11C. However, some semicontinuous particles or film-like phases can be found again on the crack surfaces of the weld with 0.047% Ce—Figs. 7E and 7F. The EPMA analysis reveals that some of the particles are enriched with S and Ce, while some are enriched only with Ce—Fig. 9. The EPMA did not show significant segregation of other elements; therefore, these segregated particles are cerium sulfides and oxides.

As can be seen from Fig. 7G, there are

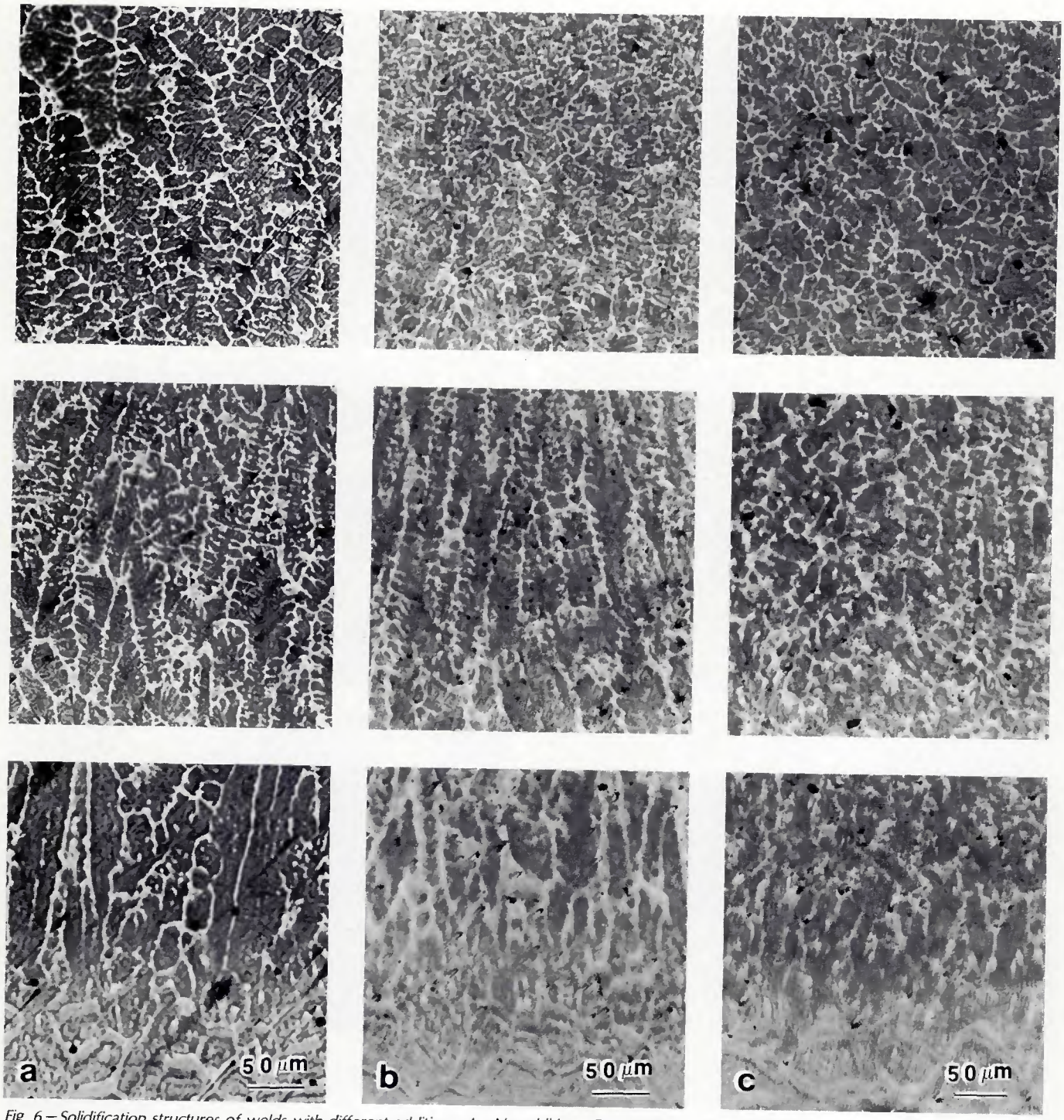

Fig. 6 — Solidification structures of welds with different additions. A — No additions; B — 0.014% Ce; C — 0.044% Ti

several irregular round particles on the crack surfaces of the weld with 0.044% Ti. The SEM/EDS analyses indicate that these particles have high S, Ti, Fe and Mn contents — Fig. 8C. The TEM and STEM/EDS analyses of the weld are shown in Figs. 10C and 11D. On the crack surfaces of the weld with 0.11% Ti, some interdendritic phases with flower patterns can be found (Fig. 7H), and they have high S and Ti contents — Fig. 8D. The TEM analysis shows that there are continuous and semicontinuous interdendritic phases in the weld with 0.11% Ti — Figs. 10D and 12. The STEM/EDS analyses indicate that these interdendritic phases are enriched with S, Ti and Mn — Fig. 12. By selected area and convergent beam diffraction analysis, it was established that at least some of the particles are TiO. The interdendritic films and semicontinuous particles in the weld with high Ti are TiS combined with TiO, and possibly have an even more complex composition.

Discussion

Base Metal Response

From the previously described analysis, it is obvious that the interdendritic films are the main factor responsible for the susceptibility of the weld in the Cr-Mo-V rotor steel to hot cracking. The high level of S results in interdendritic sulfide films during solidification, for example, from the FeS-Fe and FeS-MnS systems (Ref. 5).

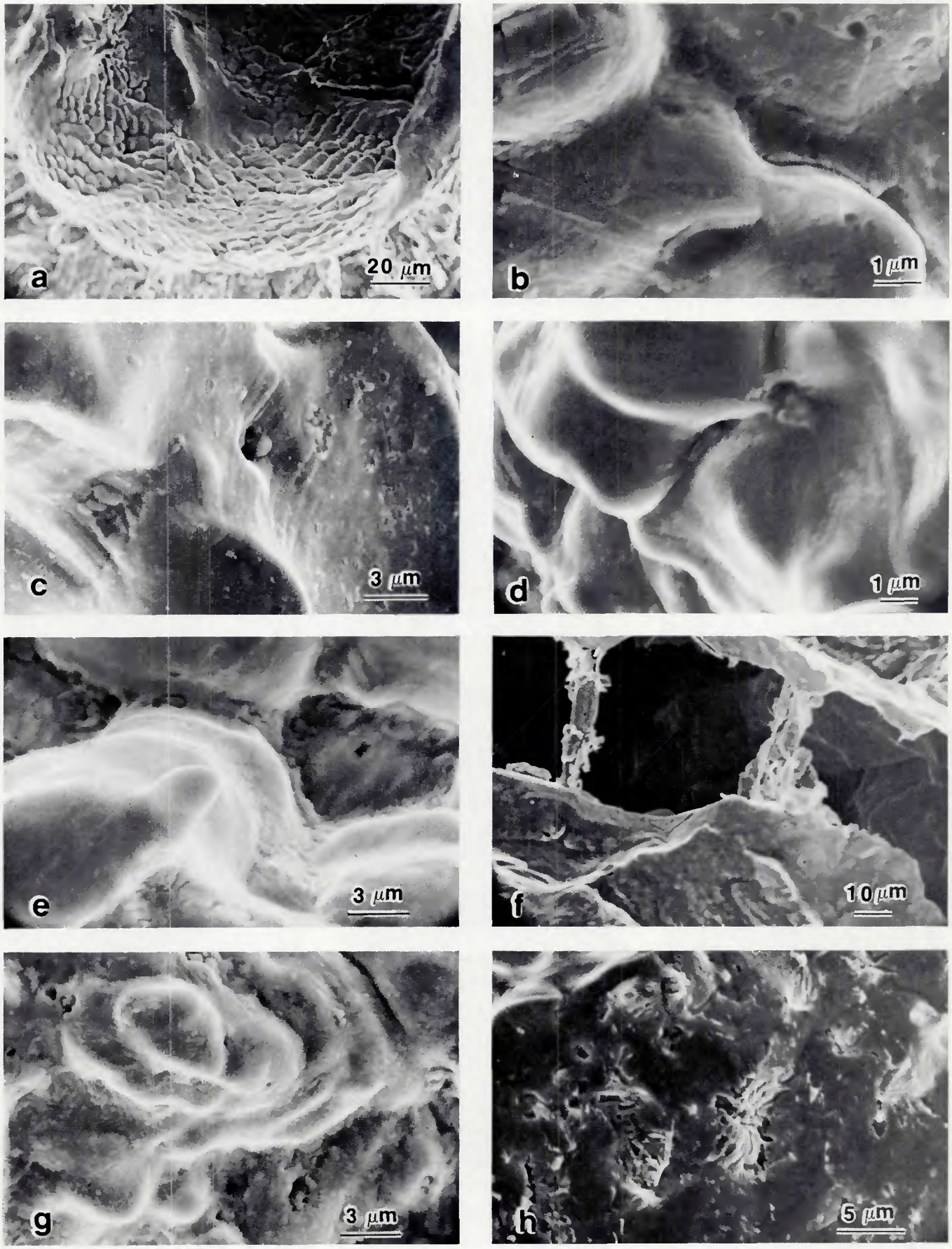

Fig. 7—SEM micrographs of interdendritic phases found at the crack surfaces of the welds. A and B—No additions; C and D—0.014% Ce; E and F—0.047% Ce; G—0.044% Ti; H—0.11% Ti

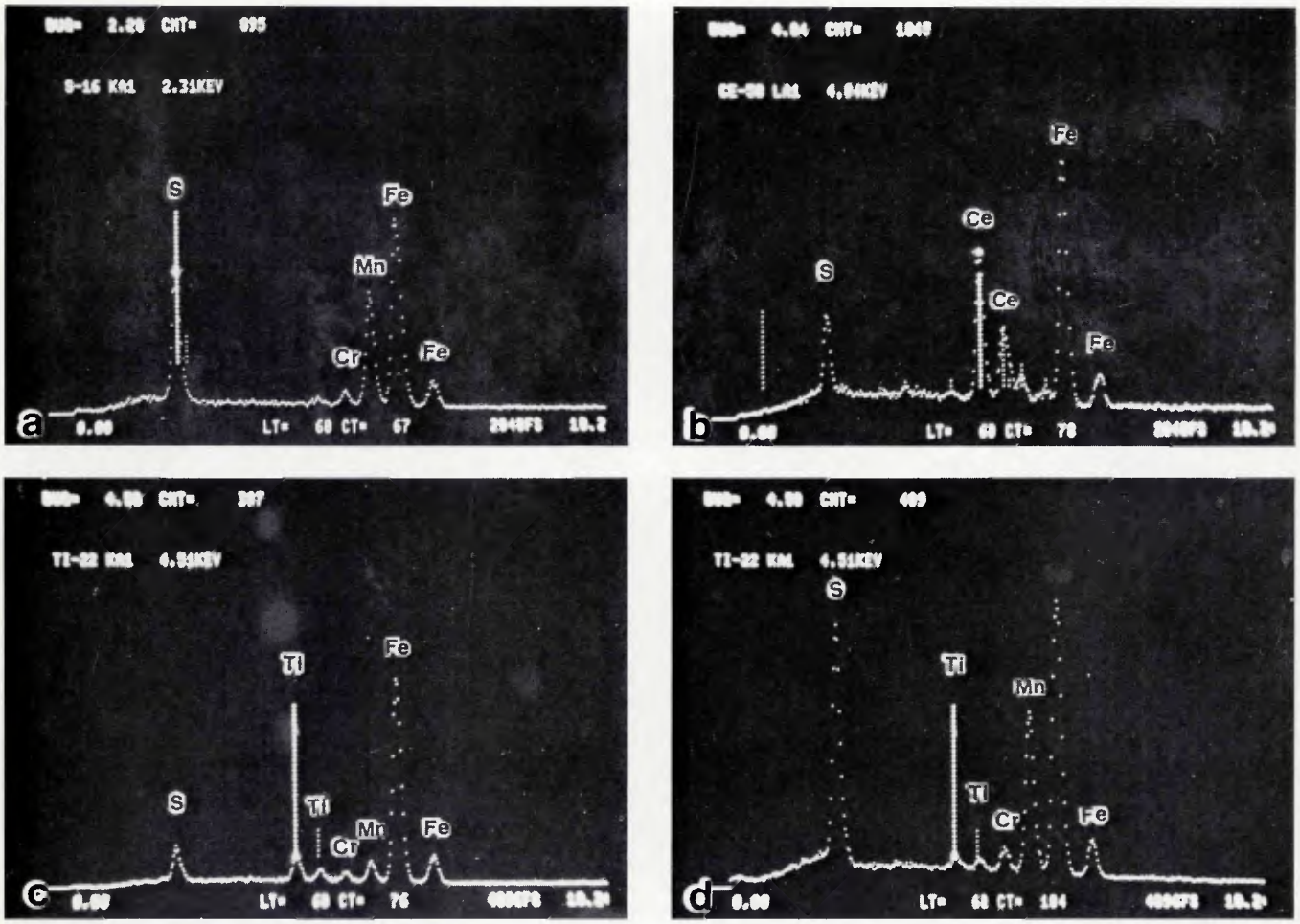

Fig. 8 — SEM/EDS spectra from the interdendritic phases found at crack surfaces of the welds. A — No additions (shown in Fig. 7B); B — 0.014% Ce (shown in Fig. 7D); C — 0.044% Ti (shown in Fig. 7G); D — 0.11% Ti (shown in Fig. 7H)

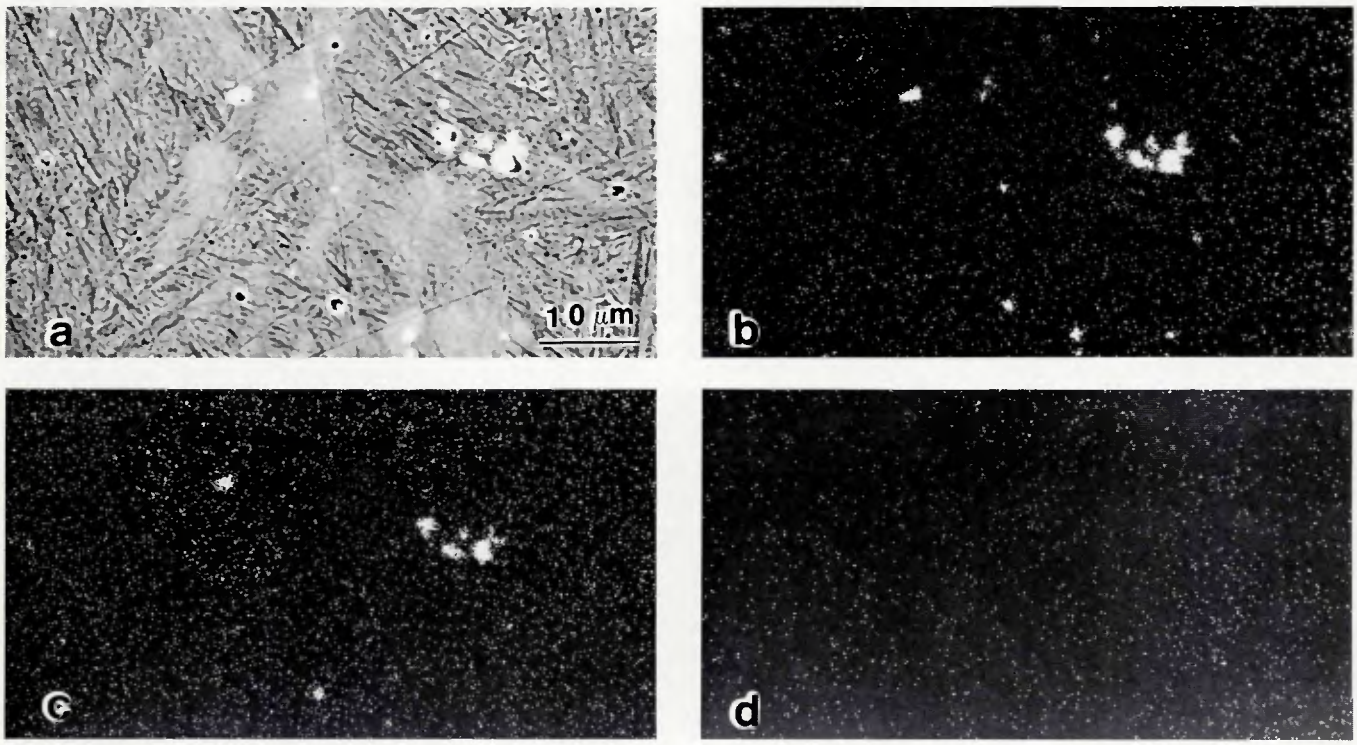

Fig. 9 — Results of the EPMA x-ray mapping of interdendritic phases in welds with 0.047% Ce. A — Backscattered image; B — Ce distribution map; C — S distribution map; D — P distribution map

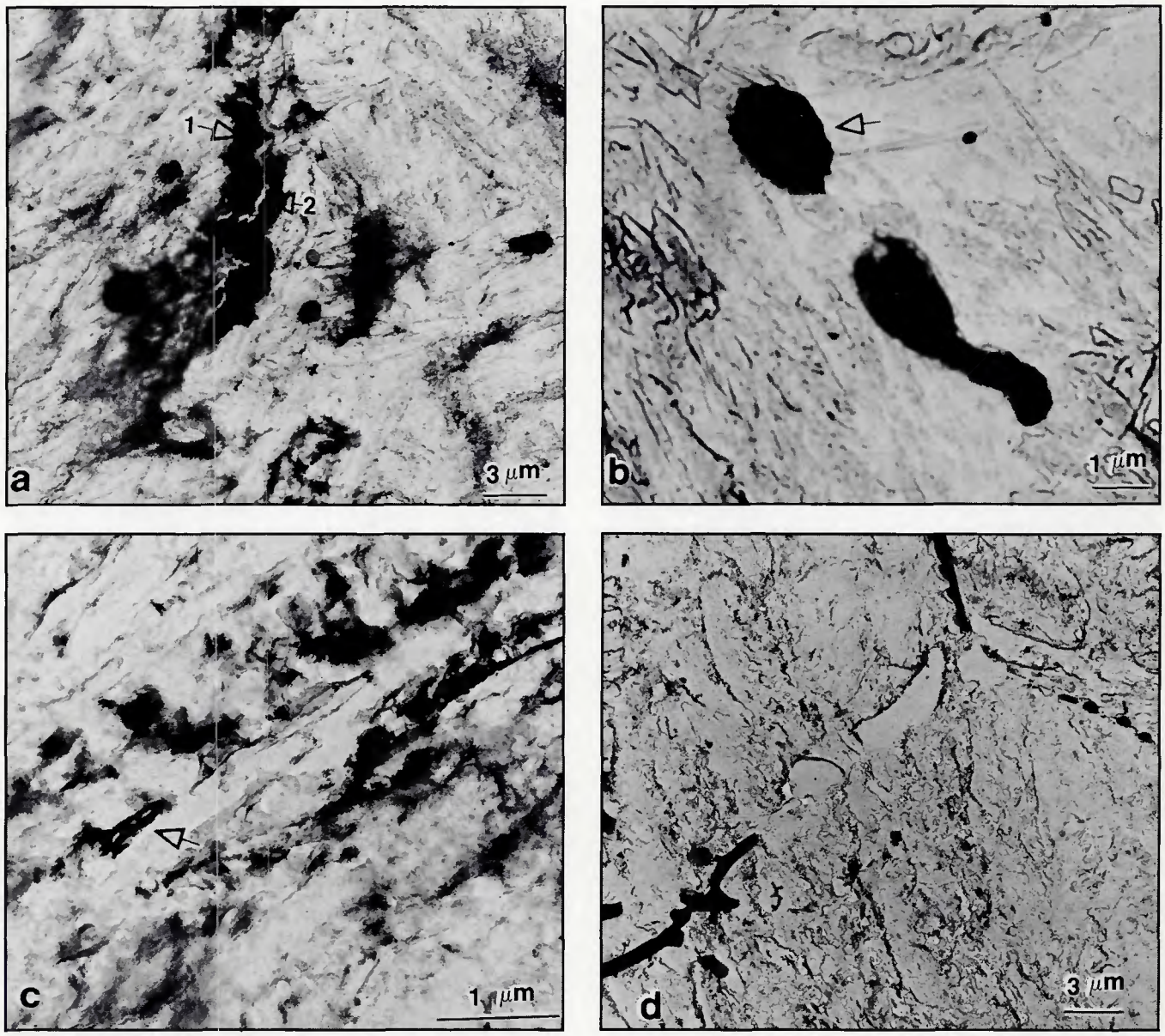

Fig. 10—TEM micrographs of interdendritic phases in the welds with different additions. A—No additions; B—0.014% Ce; C—0.044% Ti; D—0.11% Ti

C, which is relatively high, is also present and is known to promote hot cracking. Moreover, P and some low-melting impurities, for example Sn, which is 0.13 wt-% in the steel, can also increase susceptibility. The key to control of the hot cracking lies in controlling the morphology, distribution and characteristics of the intergranular phases. The present work demonstrates that alloy additions can be helpful for this purpose.

Effects of Ce and Ti on the Cr-Mo-V Welds

The effects of Ce and Ti in the weld of the Cr-Mo-V steel are manifested in three ways.

1) It produces refinement of the crystallization structure of the weld. It is known from Fig. 4 that the average value of primary dendrite arm spacing in the weld with 0.014% Ce is reduced approximately 24% from the value for welds without additions. Figure 5 shows that Ti can also refine the crystallization structure.

2) It results in modification of the morphology of the interdendritic phases. By comparing Figs. 7C, D and G with 7B, it is clear that the morphology of the phases has changed from film-like to globular or rod-like in welds with 0.014% Ce or with 0.044% Ti. Cerium is known as a sulfide shape-control element, since its sulfides are thermodynamically more stable than iron sulfides (Ref. 6) and have a high melting point (Ref. 7). On the other hand, the beneficial effect of Ti on the morphology of intergranular phases seems to be in its refinement function.

3) It produces self-segregation of Ce and Ti at interdendritic regions. In the welds with 0.047% Ce or 0.11% Ti, some film-like or semicontinuous interdendritic phases appear again—Figs. 6E, F, H, 9D and 11. They have high Ce or Ti content and are most probably sulfides and oxides of these elements.

The first two functions are beneficial, but the third one, self-segregation of Ce and Ti at grain boundaries, is harmful. These conflicting effects predict that there must be optimum ranges for Ce and Ti additions. This has been observed in this investigation. The effects of Ce and Ti on mechanical properties, arc stability and bead appearance should also be taken into account when considering the application of such additions. Fortunately,

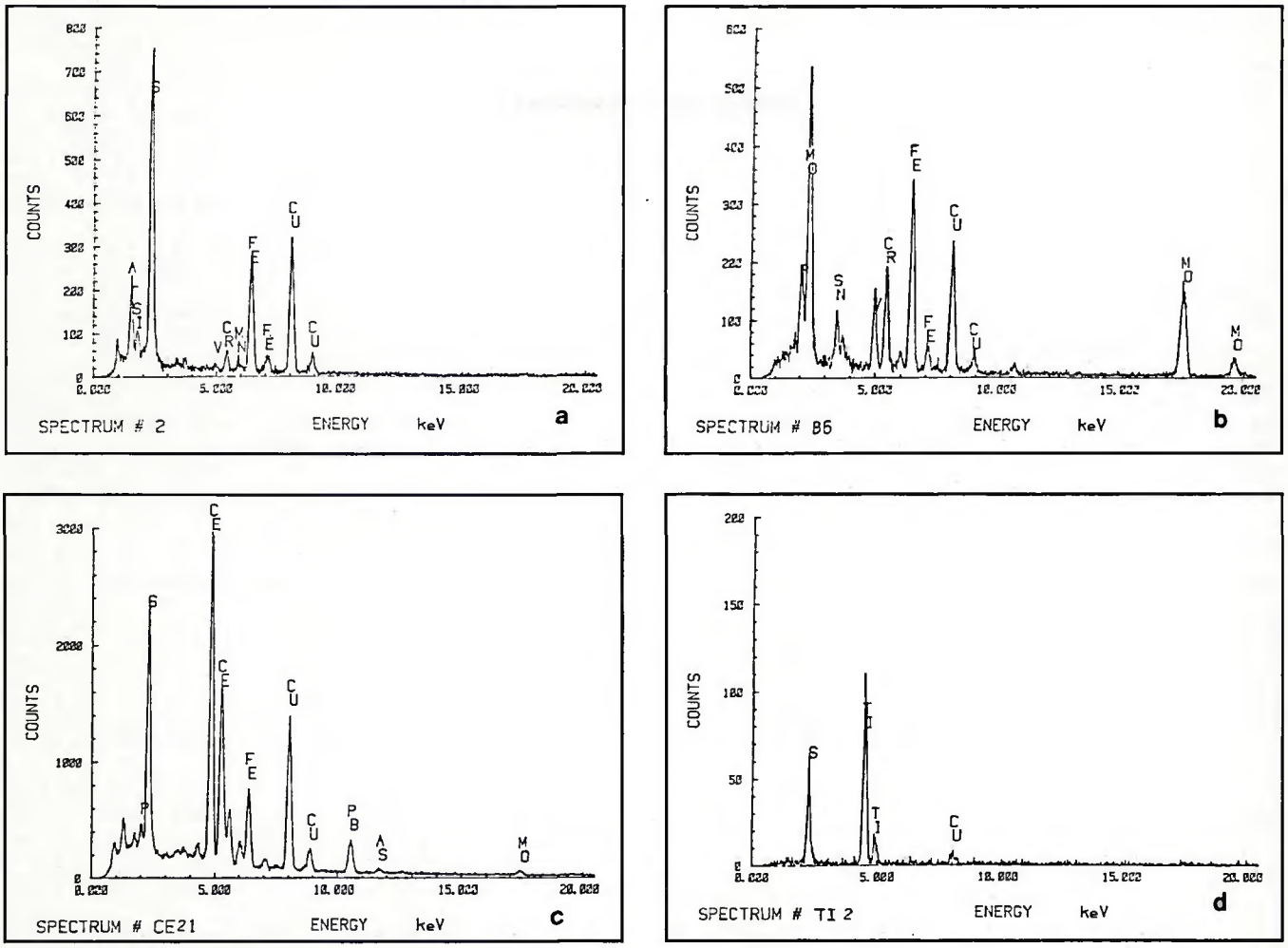

Fig. 11 — STEM/EDS spectra from the interdendritic phases in the welds. A and B — No additions (Arrows 1 and 2 in Fig. 10A); C — 0.014% Ce (arrow in Fig. 10B); D — 0.44% Ti (arrow in Fig. 10C)

within the optimum ranges corresponding to the most beneficial level for hot cracking resistance, Ce and Ti have no known harmful effects (Refs. 8–12).

Conclusions

The results of this investigation have led to the following conclusions:

1) The segregation of sulfur and carbon to interdendritic regions and the formation of film-like interdendritic phases are the main factors responsible for the susceptibility to hot cracking in the welds of the rotor Cr-Mo-V steel. Other low-melting impurity elements may play a role also.

2) Cerium and titanium in the welds of the Cr-Mo-V have the following three effects: (a) refinement of the crystallization structure, (b) modification of the interdendritic phases and (c) self-segregation at the intergranular region. Since the first two effects reduce hot cracking while the last one promotes it, the effects of these additions are not monotonic.

3) Based on the test results, the optimum ranges of cerium and titanium additions in this steel are 0.01–0.03% for

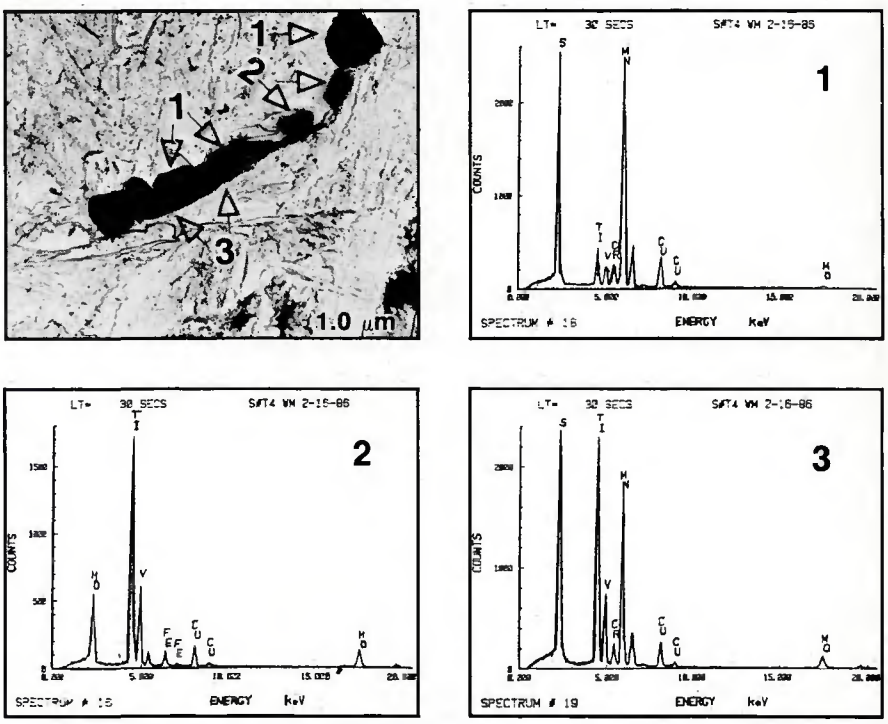

Fig. 12 — TEM micrograph and STEM/EDS spectra from a group of complex sulfide and oxide particles in the welds with 0.11% Ti

cerium and 0.03–0.06% for titanium. Within these ranges, cerium and titanium reduce susceptibility to hot cracking without any reported deleterious effects on arc characteristics or harmful changes to other properties.

Acknowledgments

The authors are grateful to Dr. R. D. Stout and to Dr. S. Lathabai for their assistance and help in the work. The assistance by the Bethlehem Steel Corporation with chemical analysis is appreciated. The authors would also like to thank the American Electric Power Co., the Delmarva Power and Light Company, the Public Service Electric and Gas Research Corp., the Pennsylvania Power and Light Co., and Northeast Utilities for contributions of materials and financial support for part of the research.

References

1. Somers, B. R., Warnock, A. S., and Pense, A. W. 1988. Weld repair and rehabilitation of turbine rotors. *Proceedings, International Conference on Life Extension and Assessment,* The Hague, Netherlands.

2. Ratz, G. A., Nippes, E. F., Matthew, J., and Baek, W. H. 1984. The weldability of sulfides shape controlled linepipe and HSLA steels. *Welding Journal* 63(11):333-s to 338-s.

3. Savage, W. F., and Lundin, C. D. 1965. The Varestraint test. *Welding Journal* 44(10):433-s to 442-s.

4. Abrams, H. Practical applications of quantitative metallography-stereology and quantitative metallography. Symposium, 74th Annual Meeting, American Society for Testing and Materials, pp. 138–184.

5. Killing, R., Thier, H., and Burat, F. 1983. Contribution to hot crack formation in C-Si and Mn alloyed weldments. Paper 13, International Conference on Welding, The Welding Institute, London, U.K.

6. Gschneidner, K. A. 1974. Thermodynamic stability and physical properties of metallic sulfides and oxysulfides. *Sulfide Inclusions in Steel.* ASM International, pp. 159–177.

7. Topp, N. E. 1965. *The Chemistry of Rare Earth Elements.* Elsevier Publishing Co.

8. Wilson, W. G. 1971. Reduced heat-affected zone cracking and improved base metal impacts through sulfide shape control with rare earth additions. *Welding Journal* 50(1):42-s to 46-s.

9. Comstock, G. F. 1955. *Titanium in Iron and Steel.* John Wiley and Sons, Inc., New York, N.Y.

10. Koubaki, A. H., North, T. H., and Bell, H. H. Properties of submerged arc deposits. *Metal Construction* 11(12):639–642.

11. Matsuyama, J., and Tsuboi, J. 1979. CO_2 arc weldability of rare earth calcium treated linepipe steels. *Report UTR79024,* Research Laboratories, Kawasaki Steel Corp., Japan.

12. Agusta, K., Nishiyama, N., and Tsuboi, J. 1981. MIG welding with pure argon shielding. *Metal Construction* 13(9):570–574.